

## Combining High Electron Affinity and Intramolecular Charge Transfer in 1,3-Dithiole–Nitrofluorene Push–Pull Diads\*\*

Dmitrii F. Perepichka,<sup>[a]</sup> Igor F. Perepichka,<sup>[b, c]</sup> Oleksandr Ivasenko,<sup>[a]</sup> Adrian J. Moore,<sup>[c, f]</sup> Martin R. Bryce,<sup>[c]</sup> Lyudmila G. Kuz'mina,<sup>[d]</sup> Andrei S. Batsanov,<sup>[c]</sup> and Nikolai I. Sokolov<sup>[e]</sup>

**Abstract:** Attaching electron-rich 1,3-dithiol-2-ylidene moieties to polynitrofluorene electron acceptors leads to the formation of highly conjugated compounds **6** to **11**, which combine high electron affinity with a pronounced intramolecular charge transfer (ICT) that is manifested as an intense absorption band in their visible spectra. Such a rare combination of optical and electronic properties is beneficial for several applications in optoelectronics. Thus, incorporation of fluorene–dithiole derivative **6a** into photoconductive films affords photothermoplastic storage

media with dramatically increased photosensitivity in the ICT region. A wide structural variation of the dithiole and fluorene parts of the molecules reveals excellent correlation between the ICT energy and the reduction potential with the Hammett's parameters for the substituents. Although only a small solvatochromism of the ICT band was ob-

served, heating the solution led to a pronounced blueshift, which was probably as a result of increased twisting around the C9=C14 bond that links the fluorene and dithiole moieties. X-ray crystallographic analysis of **7a**, **8a**, **10a**, **11a** and **13a** confirms an ICT interaction in the ground state of the molecules. The C9=C14 double bond between the donor and acceptor is substantially elongated and its length increases as the donor character of the dithiole moiety is enhanced.

**Keywords:** charge transfer • donor–acceptor systems • electron-deficient compounds • photoconductive materials • redox chemistry

[a] Prof. D. F. Perepichka, O. Ivasenko  
Department of Chemistry, McGill University  
801 Sherbrooke Street West, Montreal H3A 2K6, QC (Canada)  
Fax: (+1) 514-398-3797  
E-mail: dmitrii.perepichka@mcgill.ca

[b] Dr. I. F. Perepichka  
Centre for Materials Science  
Faculty of Science and Technology  
University of Central Lancashire  
Preston PR1 2HE (UK)  
Fax: (+44) 1772-89-4981  
E-mail: iperepichka@uclan.ac.uk


[c] Dr. I. F. Perepichka, Dr. A. J. Moore, Prof. M. R. Bryce,  
Dr. A. S. Batsanov  
Department of Chemistry, Durham University  
South Road, Durham DH1 3LE (UK)  
Fax: (+44) 191-384-4737  
E-mail: m.r.bryce@durham.ac.uk

[d] Dr. L. G. Kuz'mina  
Institute of General and Inorganic Chemistry  
Russian Academy of Sciences  
Moscow 119991 (Russian Federation)

[e] N. I. Sokolov  
Laboratory of Holography, Faculty of Natural Sciences  
University "Kievo-Mogilyanskaya Academy"  
Kiev 04145 (Ukraine)

[f] Dr. A. J. Moore  
University of Sunderland, Fleming Building  
Wharnclyffe Street, Sunderland SR1 3SD (UK)

[\*\*] Electron Acceptors of the Fluorene Series, Part 15; for Part 14 see: D. F. Perepichka, M. R. Bryce, I. F. Perepichka, S. B. Lyubchik, N. Godbert, C. A. Christensen, A. S. Batsanov, E. Levillain, E. J. L. McInnes, J. P. Zhao, *J. Am. Chem. Soc.* **2002**, *124*, 14227–14238

 Supporting Information for this article is available on the WWW under <http://www.chemistry.org> from the authors. It contains the thermochromic behaviour of **11a**; additional correlation plots; orbital energy diagrams for compounds **8** and **11**; colour versions of Figures 3, 4, and 7; <sup>1</sup>H NMR of **9a**; the results of elemental and mass spectral analyses for compounds **6** to **11**; and their DFT optimised geometries (XYZ coordinates).

## Introduction

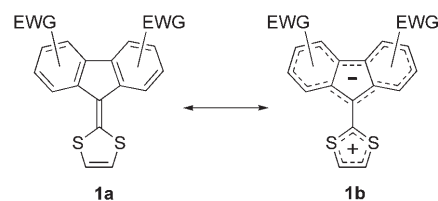
Conjugated donor- $\pi$ -acceptor molecules (D- $\pi$ -A) with strong electronic coupling between the D and A moieties have been of general interest for a number of electronic and optoelectronic applications. Large second-order polarisability and electro-optic effects render them the most promising non-linear optical and electro-optical materials for telecommunications.<sup>[1-4]</sup> More elaborate structures in this family (usually incorporating several D- $\pi$ -A moieties) have been explored for their large two- and three-photon absorption cross-sections,<sup>[5-7]</sup> which are important properties for several applications, such as optical limiting and fluorescent imaging. Recently, D- $\pi$ -A derivatives have also been extensively studied in molecular electronics, particularly for use as unimolecular rectifiers.<sup>[8,9]</sup>

Donor-acceptor (HOMO-LUMO) interactions in such molecules usually result in intramolecular charge-transfer (ICT) absorption bands in the visible or near-IR region of their electronic spectra. The strong sensitivity of the ICT band to variations in the molecular structure and media makes D- $\pi$ -A compounds convenient model systems in physical organic chemistry. Thus, solvatochromism in one such molecule, the dye 4-hydroxyphenylpyridinium, was used to establish the solvent polarity scale  $E_T$ . At the same time, a strong HOMO-LUMO interaction in the majority of such molecules makes them neither strong electron donors nor acceptors. It is, however, desirable for several applications to combine a pronounced electron affinity and strong light absorption in the same compound. A possible approach to achieve this combination would be to use a  $\pi$ -extended electron-acceptor moiety with numerous electron-withdrawing substituents, which could maintain an electron-deficient character in the presence of the ICT interaction.

Electron acceptors in the fluorene series are known for their unique ability to sensitise photoconductivity of poly-*N*-vinylcarbazole-type (PVK) semiconductive polymers and related amorphous hole-transporting materials.<sup>[10-13]</sup> The process is based on the formation of a charge-transfer complex (CTC) between the fluorene acceptor and a carbazole donor, which is highly efficient because of the great structural similarity between these components. However, the relatively weak intensity of the charge-transfer band ( $\epsilon \sim 1000\text{--}2000\text{ M}^{-1}\text{ cm}^{-1}$ <sup>[14]</sup>) affects the efficiency of the photosensitisation. Some improvements in photosensitisation were found when a nitrofluorene was covalently linked to a fullerene acceptor with an intrinsic absorption in the visible region.<sup>[15]</sup> CTCs of dendrimers that contain nitrofluorene and carbazole were used to design columnar liquid crystals with improved charge-transport characteristics.<sup>[16]</sup> Very recently, a trinitrofluorenone acceptor moiety was used together with a hexabenzocoronene donor core to build supramolecular nanotubes with substantial axial photoconductivity.<sup>[17]</sup> The electron affinity of the strongest fluorene acceptor, 9-dicyanomethylene-2,4,5,7-tetranitrofluorene, is close to that of 7,7,8,8-tetracyano-*p*-quinodimethane (TCNQ); moreover, 9-dicyanomethylene-polynitrofluorenes have up to four rever-

sible reduction waves in cyclic voltammetry (CV) experiments, which reveals their extraordinary electron-acceptor capacity.<sup>[18]</sup> The 1,3-dithiole heterocyclic ring, a structural element of the famous  $\pi$ -electron donor tetrathiafulvalene (TTF), is also a promising building block for different types of supramolecular systems and a terminal donor moiety in D- $\pi$ -A non-linear optical chromophores.<sup>[19]</sup>

We suggested that combining these two structural blocks (dithiole and nitrofluorene) would yield D- $\pi$ -A molecules with interesting electronic properties. An important feature of such a combination is that full intramolecular charge transfer, which results in a zwitterionic state D<sup>+</sup>- $\pi$ -A<sup>-</sup>, would cause aromatisation of both donor and acceptor moieties (6 and 14e systems, respectively; resonance structure **1b**). This aromatisation would stabilise the charge-separated excited state, which is of paramount importance for optoelectronic applications. The electronic properties of such diads could be tuned across a wide range by the synthetically convenient introduction of electron-donating and electron-withdrawing groups (EDG and EWG, respectively).

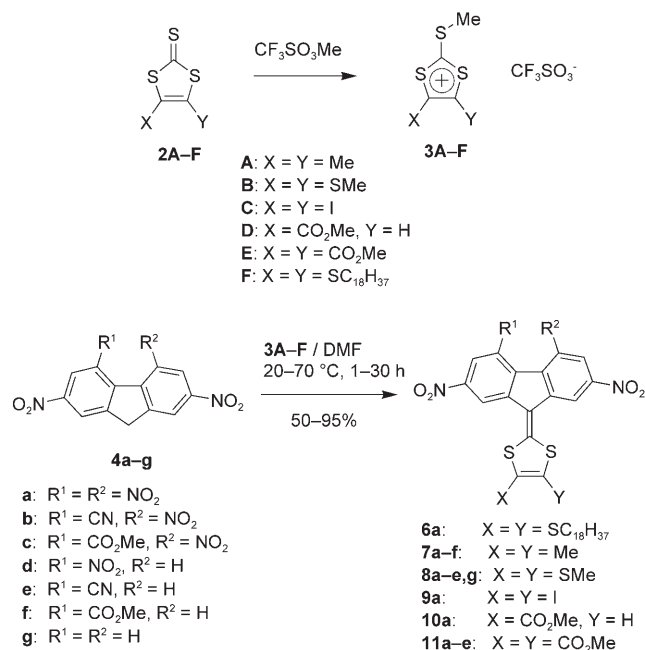


Previously we reported some representatives of the general structure **1** and showed their ability to sensitise the photoconductivity of polymers that contain carbazole.<sup>[20,21]</sup> The present work describes the synthesis and detailed studies of the structural effects in both fluorene and dithiole rings on the spectral and electrochemical properties of these new donor-acceptor diads, as well as on their supramolecular organisation in the solid state. Electrochemical and spectroscopic data have been supported by theoretical DFT calculations. We also demonstrate the remarkable stability and great potential of these materials in optoelectronic applications, that is, very high efficiency of these compounds as sensitisers of the conductivity of poly[*N*-(2,3-epoxypropyl)carbazole] (PEPK) in optical data storage processes (e.g., photothermoplastic hologram recording<sup>[11,22]</sup>).

## Results and Discussion

**Synthesis:** Nitrosubstituted fluorenes **4a-g** have been prepared by nitration of fluorene or its 4-substituted derivatives with nitric acid, or a mixture of nitric acid with acetic or sulfuric acids, as previously described.<sup>[20,23-25]</sup> As strong C-H acids,<sup>[26]</sup> derivatives **4a-g** readily participate in condensation reactions with various electrophiles, which include aldehydes,<sup>[4b,27]</sup> amides,<sup>[26]</sup> and dithiolium salts.<sup>[20,21,28]</sup> Thus, treatment of nitrosubstituted fluorenes **4a-g** with dithiolium salts

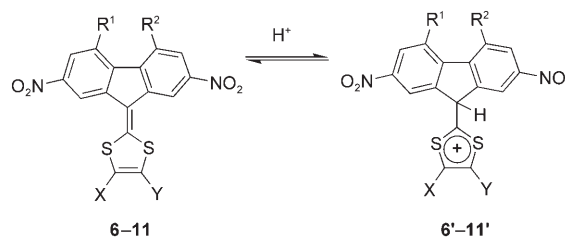
**3A–F**, which were obtained by methylation of the corresponding 1,3-dithiol-2-thiones **2A–F** with methyl trifluoromethanesulphonate,<sup>[29]</sup> results in the formation of 9-(1,3-dithiol-2-ylidene)fluorenes **6–11** (Scheme 1). The reaction proceeds



Scheme 1. Synthesis of 9-(1,3-dithiol-2-ylidene)fluorenes **6** to **11** by condensation of nitrofluorenes **4** with dithiolium salts **3**.

smoothly in *N,N*-dimethylformamide (DMF) with no additional catalyst (in contrast with common base-catalysed reactions of activated methylene compounds) and its rate positively correlates with the electron-withdrawing strength of substituents in the fluorene nucleus. Thus, for **4a** the reaction is completed within 1 h at room temperature, whereas **4g** typically requires over 24 h at 65 to 70 °C. Compounds **6** to **11** are very intensely coloured (red to black), air- and light-stable solids. No signs of decomposition were observed after storage for several years on the bench or after heating to the melting points (typically, above 250–300 °C).

Compounds **7** to **11** have a limited solubility in most organic solvents (moderate for derivatives that contain carbomethoxy substituents). Thus, long-chain-substituted derivative **6a** was specifically synthesised to improve the processability for device applications. Compounds **7** to **11**, however, all dissolve in concentrated sulfuric and trifluoromethanesulfonic acids. This results in a reversible protonation of the molecules at the C9 position of the fluorene nucleus to form cations **6'** to **11'**, which have a positive charge delocalised over an aromatic dithiolium ring<sup>[30]</sup> (Scheme 2).<sup>[20]</sup> Similar behaviour was demonstrated by other 1,3-dithiole derivatives, notably TTFs.<sup>[31]</sup> Such protonation eliminates the prerequisite conditions for ICT (donor character of the dithiole moiety, conjugation path), which affords **6'** to **11'** as almost colourless salts with UV/Vis absorption spectra that resemble



Scheme 2. Protonation of 1,3-dithiol-2-ylidene-fluorene conjugates **6** to **11** in strong acids.

ble those of the corresponding 9H-fluorenes (Figure 1). Reducing the acidity of the solution shifts the equilibrium towards non-protonated forms **6** to **11** (Scheme 2), which leads

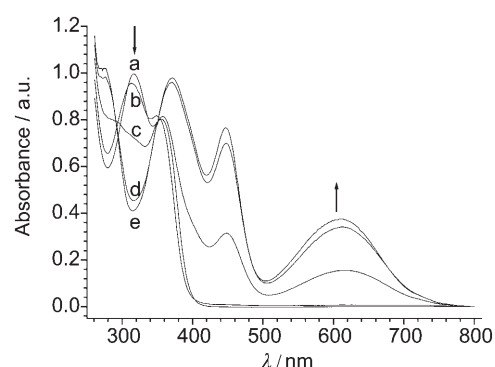


Figure 1. Electronic absorption spectra of **7a** in mixtures of H<sub>2</sub>SO<sub>4</sub>/acetic acid with various concentrations of H<sub>2</sub>SO<sub>4</sub>, a) 94, b) 62, c) 45, d) 35 and e) 29% H<sub>2</sub>SO<sub>4</sub>. The absorbance is corrected for the dilution.

to a gradual restoration of the ICT bands upon dilution of the solution in H<sub>2</sub>SO<sub>4</sub> with acetic acid (Figure 1). The basicity of diads **6** to **11** decreased with the increasing electron-withdrawing ability of substituents X and Y, which destabilises the dithiolium cation. For dicarbomethoxy-substituted **11a** only a partial protonation was observed in concentrated H<sub>2</sub>SO<sub>4</sub>, as revealed by a residual ICT absorption in the UV/Vis spectra. The protonation can be followed by a downfield shift of the proton signals in the NMR spectra. For partially protonated compound **11a**, two sets of signals that correspond to the neutral and protonated forms, were observed (see the NMR spectroscopy data given in Table 8).

**Electrochemistry:** The electrochemical behaviour of compounds **6** to **11** was studied by CV in either dichloromethane or *N,N*-dimethylacetamide (DMA) with 0.1 M Bu<sub>4</sub>NPF<sub>6</sub> as the supporting electrolyte. The presence of both electron-acceptor (nitrofluorene) and electron-donor (dithiole) fragments gives compounds **6** to **11** highly amphoteric multiredox behaviour, with up to four single-electron reduction waves (the first two or three reduction processes are reversible) and up to two single-electron oxidations (Figure 2, Table 1). It is quite unusual for organic molecules to show

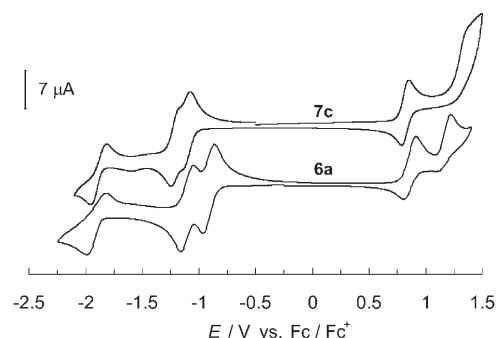


Figure 2. Cyclic voltammograms for tetranitro derivative **6a** and trinitro-carbomethoxy derivative **7c** in  $\text{CH}_2\text{Cl}_2$  that contains 0.1 M  $\text{Bu}_4\text{NPF}_6$  (scan rate  $100 \text{ mV s}^{-1}$ ).

five to seven distinct redox states (neutral, radical anion, dianion, radical trianion, tetraanion, radical cation and dication), although other examples (fullerenes, D-σ-A diads) are known.<sup>[32]</sup>

The observed first and second reduction potentials are in good linear correlation with the sum of the Hammett constants of the substituents in the benzene rings of the fluorene moiety ( $\sigma_p^A$ ) as shown by Equation (1), (Figure 3).

$$E_{1/2} = E_{1/2}^0 + \rho^A \sum \sigma_p^A \quad (1)$$

in which  $E_{1/2}$  is the observed half-wave redox potentials,  $E_{1/2}^0$  is the  $E_{1/2}$  value of the reference compound (unsubstituted benzene rings in the fluorene nuclei,  $\sum \sigma_p^A = 0$ ), and  $\rho^A$  is a sensitivity parameter of the redox potential to substituents effects.

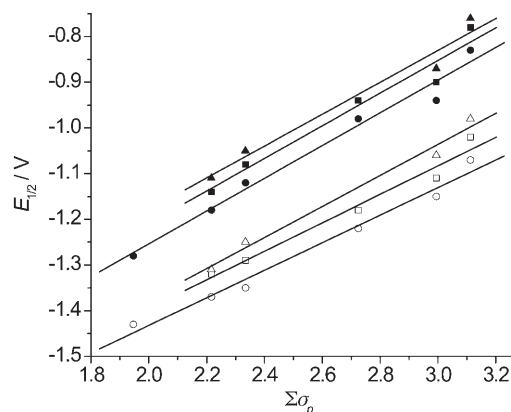


Figure 3. Dependence of the  $E_{1/2}^{\text{red1}}$  (filled shapes) and  $E_{1/2}^{\text{red2}}$  (open shapes) reduction potentials of series **7** (circles), **8** (squares) and **11** (triangles) versus the sum of the  $\sigma_p$  constants in the fluorene moiety. Lines show the linear fits of the experimental data from Table 1 (for correlation parameters see Table 2).

The potentials  $E_{1/2}^{\text{red1}}$  and  $E_{1/2}^{\text{red2}}$  both showed good linear correlations (correlation coefficient  $r=0.980\text{--}0.993$ ) on  $\sum \sigma_p^A$  with sensitivity parameters of  $\rho^A \approx 0.35$  for red1 and  $\approx 0.30$  for red2 processes (Table 2). The  $\rho^A$  values were essentially independent of the substituents in the dithiole ring (cf. series **7**, **8** and **11**; Table 2), which means that there is no cross-correlation between the variations of the fluorene and the dithiole structures.

In the reduced (anionic) states, the negative charge should be localised almost exclusively on the fluorene fragment, which is also in agreement with LUMO orbital localisation on the fluorene moiety (see the Theoretical studies

Table 1. CV data for solutions of compounds **6** to **11** in DMA and  $\text{CH}_2\text{Cl}_2$ .<sup>[a]</sup>

	Solvent	$E_{1/2}^{\text{ox1}}$ (D <sup>+</sup> →D <sup>2+</sup> )	$E_{1/2}^{\text{red1}}$ (A <sup>+</sup> →A <sup>•+</sup> )	$E_{1/2}^{\text{red2}}$ (A <sup>•+</sup> →A <sup>2+</sup> )	$E_{1/2}^{\text{red3}}$ (A <sup>2+</sup> →A <sup>3+</sup> )	$E_{\text{pa}}^{\text{red4}}$ (A <sup>3+</sup> →A <sup>4+</sup> )	HOMO <sup>[b]</sup> [eV]	LUMO <sup>[b]</sup> [eV]	$K_{\text{dispr}} \times 10^{\text{d}[c]}$ [M <sup>-1</sup> ]
<b>6a</b>	$\text{CH}_2\text{Cl}_2$	0.86, 1.22 ir <sup>[d]</sup>	-0.91	-1.10	-1.91	-	-5.9	-4.1	6.0
<b>6a</b>	DMA	-	-0.80	-1.04	-2.04 <sup>[e]</sup>	-	-	-4.2	0.9
<b>7a</b>	DMA	0.85 ir	-0.83	-1.07	-2.01	-	-5.8	-4.2	0.9
<b>7b</b>	DMA	0.84 ir	-0.94	-1.15	-2.04	-	-5.8	-4.1	2.8
<b>7c</b>	$\text{CH}_2\text{Cl}_2$	0.82, 1.35 ir	-1.11	-1.21	-1.89	-	-5.8	-3.9	≈200.0
<b>7c</b>	DMA	0.79 ir	-0.98	-1.22	-2.05	-	-5.8	-4.0	0.9
<b>7d</b>	DMA	0.76 ir	-1.12	-1.35	-2.02	-	-5.8	-3.9	1.3
<b>7e</b>	DMA	0.73 ir	-1.18	-1.37	-	-	-5.7	-3.8	6.0
<b>7f</b>	DMA	-	-1.28	-1.43	-	-	-	-3.7	29.0
<b>8a</b>	DMA	0.79 ir	-0.78	-1.02	-2.00	-	-5.8	-4.2	0.9
<b>8b</b>	DMA	0.77 ir	-0.90	-1.11	-2.03	-	-5.8	-4.1	2.8
<b>8c</b>	DMA	0.75 ir	-0.94	-1.18	-2.05	-	-5.8	-4.1	1.9
<b>8d</b>	DMA	0.73 ir	-1.08	-1.29	-2.00	-	-5.7	-3.9	2.8
<b>8e</b>	DMA	0.72 ir	-1.14	-1.32	-1.53 ir	-	-5.7	-3.9	8.9
<b>9a</b>	DMA	-	-0.76	-1.01	-1.99	-	-	-4.2	0.6
<b>10a</b>	DMA	1.18 ir	-0.77	-1.02	-2.00	-	-6.2	-4.2	5.8
<b>11a</b>	DMA	-	-0.76	-0.98	-1.79	-2.08 <sup>[e]</sup>	-	-4.2	1.9
<b>11b</b>	DMA	-	-0.87	-1.06	-1.81	-2.10 <sup>[e]</sup>	-	-4.1	6.0
<b>11d</b>	DMA	-	-1.05	-1.25	-1.83	-2.03 <sup>[e]</sup>	-	-3.9	4.1
<b>11e</b>	DMA	-	-1.11	-1.31	-1.88 <sup>[e]</sup>	-	-	-3.9	4.1

[a] 0.1 M  $\text{Bu}_4\text{NPF}_6$  was used as the supporting electrolyte (scan rate  $100 \text{ mV s}^{-1}$ ). Potentials are given versus  $\text{Fc}/\text{Fc}^+$ . [b] Calculated from  $\text{MO} = -5.0 - E_{1/2}$  (vs.  $\text{Fc}/\text{Fc}^+$ ).<sup>[59]</sup> [c]  $K_{\text{dispr}}$  is the disproportionation constant in the equilibrium  $2\text{A}^{\cdot-} \rightleftharpoons \text{A} + \text{A}^{2-}$ , which was estimated from the equation for the single-electron redox process,  $\Delta E_{1/2}^{\text{red}(1-2)} = E_{1/2}^{\text{red1}} - E_{1/2}^{\text{red2}} = -0.059 \log K_{\text{dispr}}$ .<sup>[34]</sup> [d] ir: irreversible, values correspond to  $E_{\text{pa}}$ . The second value is for the  $\text{D}^{\cdot+} \rightarrow \text{D}^{2+}$  process (oxidation to dication). [e] The estimated uncertainties for these values are  $\pm 0.05 \text{ V}$ .

Table 2. Correlation parameters for the reduction potentials of compounds **7**, **8** and **11** from Equation (1).<sup>[a]</sup>

Redox process	$E_{1/2}^0$ [eV]	$\rho^A$ [V]	$r$	$s_0$	$n$
<b>7a–f</b> $E_{1/2}^{\text{red1}}$	$-1.998 \pm 0.072$	$0.366 \pm 0.027$	0.989	0.028	6
<b>7a–f</b> $E_{1/2}^{\text{red2}}$	$-2.059 \pm 0.053$	$0.308 \pm 0.020$	0.991	0.021	6
<b>8a–e</b> $E_{1/2}^{\text{red1}}$	$-1.923 \pm 0.112$	$0.354 \pm 0.041$	0.980	0.033	5
<b>8a–e</b> $E_{1/2}^{\text{red2}}$	$-2.012 \pm 0.093$	$0.307 \pm 0.029$	0.982	0.027	5
<b>11a,b,d,e</b> $E_{1/2}^{\text{red1}}$	$-1.877 \pm 0.122$	$0.348 \pm 0.046$	0.984	0.036	4
<b>11a,b,d,e</b> $E_{1/2}^{\text{red2}}$	$-2.055 \pm 0.076$	$0.339 \pm 0.028$	0.993	0.022	4

[a] The following Hammett constants were used,  $\sigma_p = 0.78$  ( $\text{NO}_2$ ), 0.66 (CN), 0.45 ( $\text{CO}_2\text{Me}$ ), 0 (SMe) and  $-0.17$  (Me);<sup>[38]</sup>  $r$  is the correlation coefficient,  $s_0$  is the standard deviation and  $n$  is the number of points used in the correlation.

section). Therefore, the sensitivity of the reduction potentials to substituents in the fluorene ring ( $\rho^A$ ) is five to ten times higher than the corresponding sensitivity to substituents in the dithiole moiety ( $\rho^D = 0.04\text{--}0.07$  V for both reduction waves).<sup>[33]</sup>

The thermodynamic stability of the radical anion versus the corresponding dianion is described by the equilibrium  $2\text{A}^{\cdot-} \rightleftharpoons \text{A}^0 + \text{A}^{2-}$  with a disproportionation constant  $K_{\text{dispr}}$ . It can be determined from CV experiments as  $E_{1/2}$  and  $K_{\text{dispr}}$  are related through Equation (2):<sup>[34]</sup>

$$E_{1/2}^{\text{red1}} - E_{1/2}^{\text{red2}} = -0.059 \log K_{\text{dispr}} \quad (2)$$

For systems with  $K_{\text{dispr}}$  values greater than  $10^{-1}$ , two redox processes coalesce into a single two-electron redox wave in CV experiments. We have previously observed a large variation in the thermodynamic stability of radical anions of fluorene-based acceptor molecules<sup>[14]</sup> as well as of radical cations of 1,3-dithiole-based donor molecules.<sup>[35]</sup> In the most extreme case, the radical cation of a  $\pi$ -extended dithiole derivative is completely destabilised, which gives rise to a truly two-electron (inverted potentials) oxidation process.<sup>[35,36]</sup> In dithiole–fluorene diads, a complete coalescence of the first and second reduction waves has never been observed, although the thermodynamic stability of species  $\text{A}^{\cdot-}$  has a slight tendency to decrease with a reduction in the electron-withdrawing character of substituents in the fluorene moiety (cf.  $K_{\text{dispr}} = 0.9 \times 10^{-4}$  for **7a** and  $29 \times 10^{-4}$  for **7f**, Table 1). A relative stabilisation of the radical anion was achieved in polar solvents; the disproportionation constant is decreased by over two orders of magnitude when low polarity  $\text{CH}_2\text{Cl}_2$  is replaced by highly polar DMA (e.g.,  $K_{\text{dispr}} = 0.9 \times 10^{-4}$  and  $200 \times 10^{-4}$  for compound **7c** in DMA and  $\text{CH}_2\text{Cl}_2$ , respectively).

A single-electron electrochemical oxidation of compounds **6** to **11** produces radical cation species, in which the positive charge is expected to mainly localise on the dithiole fragment (as the aromatic dithiolium cation) with the unpaired electron residing on the fluorene moiety. Although this type of radical was shown to be very stable in the radical anion

state (a radical ion copper salt of 2,4,5,7-tetranitro-9-dicyanomethylene-fluorene was isolated and analysed by X-ray crystallography),<sup>[37]</sup> all attempts to isolate or analyse the radical cation salts of **7** and **8** by chemical oxidation with  $\text{NOBF}_4$  have failed. Nevertheless, the above-mentioned radical cations are reasonably stable on the CV timescale in solvents such as  $\text{CH}_2\text{Cl}_2$  (Figure 2), and even the second (irreversible) oxidation peak was observed. Unfortunately, owing to the low solubility of the other derivatives, the use of highly nucleophilic DMA as the solvent was unavoidable, and only irreversible oxidation peaks have been observed in this solvent (Table 1).

**Intramolecular charge transfer: electron-absorption spectroscopy studies:** The intense colour of compounds **6** to **11** is the result of intramolecular charge transfer (ICT) from the donor dithiole moiety onto the acceptor nitrofluorene nucleus, which can be visualised by resonance structure **1b**. The ICT manifests itself in a long-wavelength absorbance band (ICT band) with maxima in the range of 470 to 610 nm and a high extinction coefficient ( $\sim 10000 \text{ M}^{-1} \text{ cm}^{-1}$ ). Not unexpectedly, increasing the electron-withdrawing strength of substituents  $\text{R}^1$  and  $\text{R}^2$  in the acceptor fluorene fragment ( $\text{H} < \text{CO}_2\text{Me} < \text{CN} < \text{NO}_2$ ) and the electron-releasing ability of substituents X and Y ( $\text{CO}_2\text{Me} < \text{I} < \text{SMe} < \text{Me}$ ) in the donor dithiole fragment results in a pronounced bathochromic shift of the ICT band. Remarkably, however, the energy of the ICT band maxima ( $h\nu_{\text{ICT}}$ , eV) is in good linear dependence with the sum of the Hammett parameters of the substituents ( $\Sigma\sigma_p$ )<sup>[38]</sup> in either acceptor [Eq. (3), see Table 3 for correlation parameters in series **7**, **8** and **11**] or donor moieties [Eq. (4), sensitivity parameter  $\rho^D = 0.226 \pm 0.030$ , correlation coefficient  $r = 0.967$ ].

$$h\nu_{\text{ICT}} = h\nu_{\text{ICT}}^0 + \rho^A \sum \sigma_p^A \quad (3)$$

$$h\nu_{\text{ICT}} = h\nu_{\text{ICT}}^0 + \rho^D \sum \sigma_p^D \quad (4)$$

The sensitivity parameters,  $\rho^A$  and  $\rho^D$ , for an acceptor and a donor series, respectively, have an opposite sign, but are of almost equal absolute value within experimental error. Thus the cross-correlation term is insignificant and the ICT energy correlates well with the  $\Sigma\sigma_p^A - \Sigma\sigma_p^D$  term [Eq. 5, Figure 4]. The correlation on Figure 4 incorporates the previously reported fluorene–dithioles series **12a–d**.<sup>[20]</sup> Such remarkably linear dependence of the  $h\nu_{\text{ICT}}$  on the substituents throughout almost the entire visible range of the spectrum ( $\lambda_{\text{max}} = 470\text{--}610$  nm) allows fine tuning of the absorption band, which is important for tailoring the sensitivity of the photoconductive materials based on these compounds (see below).

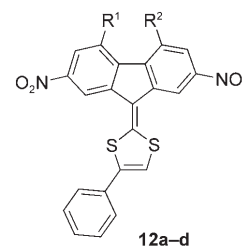




Table 3. Maxima of the ICT bands of compounds **6–11** in different solvents and correlation parameters for the series **7**, **8** and **11b** from Equation (3).

	(CH <sub>2</sub> Cl) <sub>2</sub> λ <sub>ICT</sub> [nm]	DMF λ <sub>ICT</sub> [nm]	Acetone λ <sub>ICT</sub> [nm] (ε <sub>ICT</sub> [M <sup>-1</sup> cm <sup>-1</sup> ])
<b>6a</b>	590 <sup>[a]</sup>	–	–
<b>7a</b> <sup>[b]</sup>	611	609.5	595 (8600)
<b>7b</b> <sup>[b]</sup>	589	588	–
<b>7c</b> <sup>[b]</sup>	580	582	–
<b>7d</b> <sup>[b]</sup>	554	546.5	–
<b>7e</b> <sup>[b]</sup>	540	542	–
<b>7f</b> <sup>[b]</sup>	535.5	532	–
<b>8a</b> <sup>[c]</sup>	592	589	578 (9700)
<b>8b</b> <sup>[c]</sup>	572	567	–
<b>8c</b> <sup>[c]</sup>	568	563	–
<b>8d</b> <sup>[c]</sup>	538	531.5	–
<b>8e</b> <sup>[c]</sup>	529	523.5	–
<b>8g</b> <sup>[c]</sup>	498	495	–
<b>9a</b>	558	572.5	–
<b>10a</b>	557	560	–
<b>11a</b> <sup>[d]</sup>	544	546	535 (9800)
<b>11b</b> <sup>[d]</sup>	528.5	527.5	–
<b>11c</b> <sup>[d]</sup>	520	523	–
<b>11d</b> <sup>[d]</sup>	496	495.5	–
<b>11e</b> <sup>[d]</sup>	488	–	–
<b>11g</b> <sup>[d]</sup>	472	474.5	–

[a] Recorded in CH<sub>2</sub>Cl<sub>2</sub>. [b] Correlation parameters determined by Eq. (3), in which *R* is the multiple correlation coefficient,  $hv_{ICT}^0 = (2.83 \pm 0.05)$  ((CH<sub>2</sub>Cl)<sub>2</sub>),  $(2.86 \pm 0.05)$  eV (DMF);  $\rho_A = (-0.249 \pm 0.020)$  ((CH<sub>2</sub>Cl)<sub>2</sub>),  $(-0.259 \pm 0.018)$  eV (DMF);  $R = 0.987$  ((CH<sub>2</sub>Cl)<sub>2</sub>),  $0.991$  (DMF). [c]  $hv_{ICT}^0 = (2.88 \pm 0.03)$ , ((CH<sub>2</sub>Cl)<sub>2</sub>),  $(2.91 \pm 0.04)$  eV (DMF);  $\rho_A = (-0.245 \pm 0.013)$  ((CH<sub>2</sub>Cl)<sub>2</sub>),  $(-0.248 \pm 0.017)$  eV (DMF);  $R = 0.994$  ((CH<sub>2</sub>Cl)<sub>2</sub>),  $0.990$  (DMF). [d]  $hv_{ICT}^0 = (2.99 \pm 0.05)$  ((CH<sub>2</sub>Cl)<sub>2</sub>),  $(2.95 \pm 0.07)$  eV (DMF);  $\rho_A = (-0.221 \pm 0.021)$  ((CH<sub>2</sub>Cl)<sub>2</sub>),  $(-0.208 \pm 0.025)$  eV (DMF);  $R = 0.981$  ((CH<sub>2</sub>Cl)<sub>2</sub>),  $0.978$  (DMF).

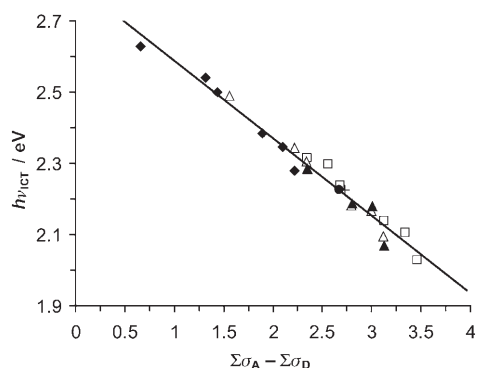


Figure 4. Cross-correlation of the first electronic transition ( $hv_{ICT}$ ) in compounds **9–12** with varying the substituents in both the fluorene and the dithiole moieties (□: series **7**, △: series **8**, ●: compound **9a**, +: compound **10a**, ◆: series **11**, ▲: series **12** (from ref. [24]). The solid line shows the linear fit according to Equation (5) (total number of points  $n = 24$ , correlation coefficient  $r = 0.993$ ).

$$hv_{ICT} = (2.81 \pm 0.02) + (-0.22 \pm 0.01) (\sum \sigma_A - \sum \sigma_D) \quad (5)$$

**Solvato- and thermochromism:** The compounds studied reveal a relatively weak solvatochromic effect of their ICT bands, in which the  $\lambda_{ICT}$  varies by less than 20 nm

( $\approx 0.05$  eV) in different solvents (Table 3). As for other push–pull fluorene derivatives, the highest wavelength absorption was observed in highly polarisable (aromatic and chlorinated) solvents, whereas the polarity of the media did not have a major effect.<sup>[27d]</sup> This suggests that there is a significant ICT in the ground state (i.e., the contribution of resonance form **1b** is high), with relatively small changes in the dipole moment of the molecules during photoexcitation. An interesting media effect is, however, a pronounced thermochromic behaviour. Solutions of compounds **6** to **11** demonstrate a hypsochromic shift of their ICT bands with increasing temperature (Figure 5). The ICT band energy is inverse-

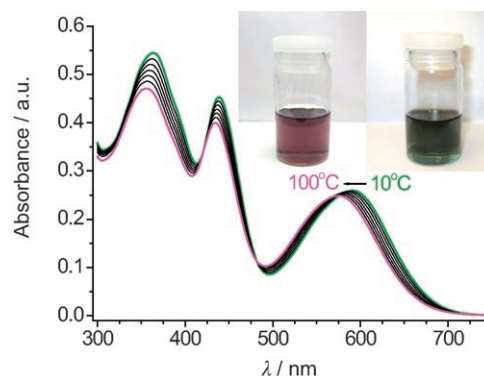


Figure 5. The effect of the temperature on the position of ICT bands in solutions of **6a** in 1,2-dichlorobenzene was observed (no correction for the solution thermal expansion was made, which led to a minor decrease in the observed absorbance with increasing temperature). The inset shows photographs of solutions in chlorobenzene at 100°C (left) and 10°C (right).

ly proportional to the temperature [Eq. (6)], and the temperature sensitivity parameters  $\alpha$  ( $-71$  for **6a** and  $-82$  eV/K for **11a** in chlorobenzene, see the Supporting Information) are very similar to those we have previously observed for other fluorene–dithiole diads.<sup>[20]</sup>

$$hv_{ICT} = hv_{ICT}^{T(\infty)} + \alpha/T \quad (6)$$

Similar behaviour is documented for conjugated oligo- and polythiophenes, for which it is explained by torsional distortions of the conjugated chain (rotation around C–C inter-unit bonds) at elevated temperatures.<sup>[39]</sup> It is likely that the increased bond length of the C9=C14 bond between the fluorene and dithiole parts of the molecule (see the section on X-ray crystallography below) facilitates the twist around this bond at elevated temperature, which, in turn, suppresses conjugation to cause a blue shift of the ICT band.

**X-ray crystallography:** To assess the structural variations in fluorene–dithiolyldiene diads, we performed X-ray crystallographic studies on derivatives **7a**, **8a** (briefly reported earlier<sup>[21]</sup>), **10a**, **11a** and **13a** (Figure 6) with the same (2,4,5,7-tetranitro-) substitution in the fluorene acceptor moiety and varied 4,5-substituents in the dithiole donor moiety. These

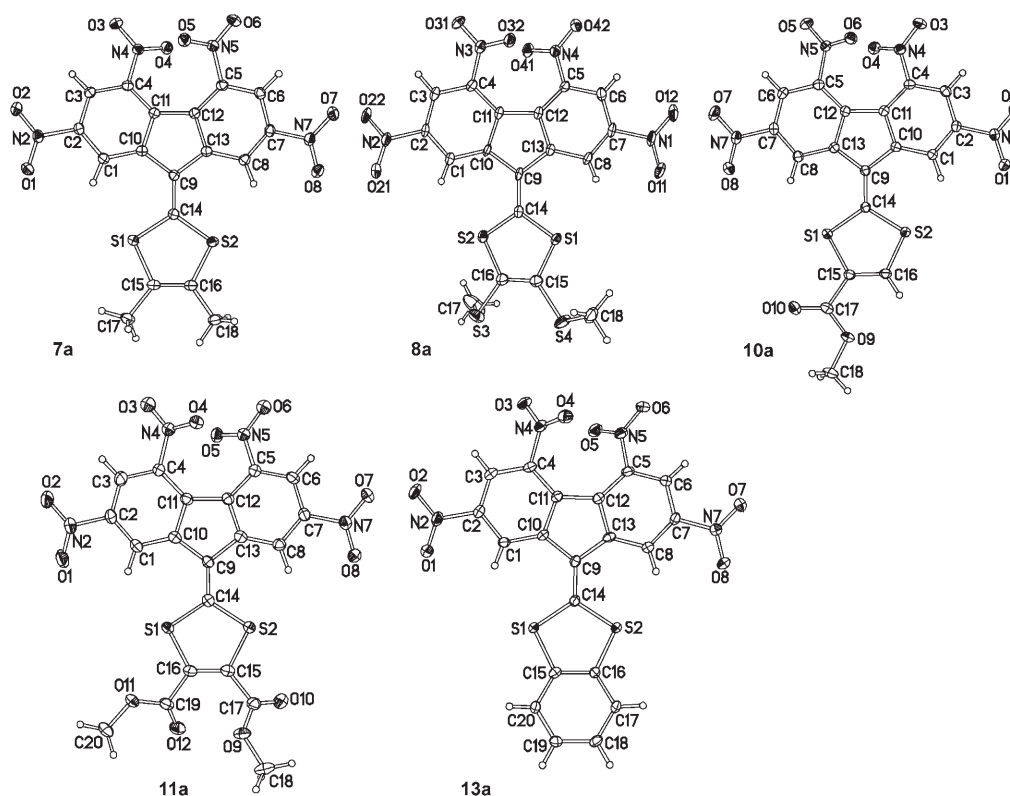


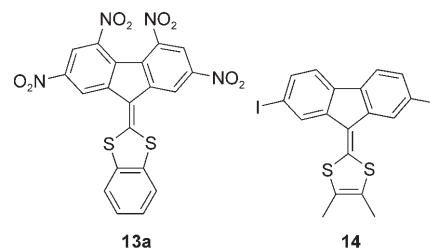
Figure 6. X-ray molecular structures of **7a**, **8a**, **10a**, **11a** and **13a**. Thermal ellipsoids are drawn at the 50% probability level. The DMSO molecule (**10a**), disorder (**11a**) and the second independent molecule of **13a** are omitted.

variations play two different roles, firstly, their electronic influence affects the distribution of the electronic density (ICT) in the molecule. The C9–C14 bond, which must be a single bond in **1b**, is indeed longer in compounds **7** to **13** than in **14** (1.367(3) Å) in which the fluorene moiety has little electron-withdrawing ability<sup>[35]</sup> (see Table 4). The lengthening (as well as the twist around this bond) is stronger when the dithiole moiety carries electron-releasing substituents (**7a**, **8a**) and weaker when it has electron-withdrawing CO<sub>2</sub>Me substituents (**10a**, **11a**), although the effect only marginally exceeds experimental error, and the C15=C16 bond distance (which must lengthen with the increase in ICT) is even less sensitive. Thus, the increased donor abil-

ity of the dithiole fragment, that is, from **11a** with two electron-withdrawing CO<sub>2</sub>Me substituents to **7a** with two electron-releasing methyl substituents, is manifested by a slight increase in the length of the C9=C14 bond from 1.376 to 1.398 Å. Therefore, the observed bond lengthening is clearly attributable to ICT, as visualised by resonance forms **1a**↔**1b**. Nevertheless, the length of this bond is still closer to a typical double bond, which suggests the neutral (non-zwitterionic) ground state of the molecules.

Table 4. Selected bond lengths [Å] from single crystal X-ray diffraction and DFT B3LYP/6-31G(d) calculations.

	C9–C14 bond		C15–C16 bond	
	X-ray	DFT	X-ray	DFT
<b>7a</b>	1.398(2)	1.3832	1.341(2)	1.3462
<b>7b</b>	–	1.3826	–	1.3462
<b>7c</b>	–	1.3808	–	1.3459
<b>7d</b>	–	1.3807	–	1.3459
<b>7e</b>	–	1.3791	–	1.3460
<b>7f</b>	–	1.3785	–	1.3455
<b>7g</b>	–	1.3762	–	1.3458
<b>8a</b>	1.395(5) <sup>[21]</sup>	1.3808	1.352(5) <sup>[21]</sup>	1.3530
<b>10a</b>	1.384(2)	1.3800	1.337(2)	1.3444
<b>11a</b>	1.376(3)	1.3801	1.339(3)	1.3508
<b>13a</b>	1.391(4)	1.3810	1.396(4)	1.3982



In each case the fluorene moiety is warped as a result of steric repulsion between the 4- and 5-nitro substituents, which (together with the C4 and C5 atoms) tilt to opposite sides of the fluorene plane. The puckering is not strong enough to disrupt the aromatic system. Molecule **11a** is disordered between two oppositely warped conformations, of which the major one (72% occupancy) is shown. Compound

**10a** crystallised as a 1:1 solvate with DMSO, which is disordered, but forms a relatively strong secondary bond S1⋯O 2.910(2) Å with **10a**. The asymmetric unit of **13a** comprises two independent molecules of similar geometry, in which the dithiole ring (planar in other molecules) is folded along the S⋯S vector by 7.4 or 2.8°. Molecule **8a** is twisted by 20° around the C9=C14 bond; this twist amounts to 6° in **7a** and 1 to 3° in other compounds. Thus the donor and acceptor moieties are almost coplanar and such a conformation favours a partial ICT, as represented by resonance forms **1a**↔**1b**.

All five crystal structures contain continuous stacks of molecules related through inversion centres (and thus are rigorously parallel) or, in **11a**, related through a glide plane and roughly parallel (within 10°). In **7a** and **8a** the stacking is mainly between acceptor moieties (A), whereas the donor groups (D) are separated as widely as possible within the stack. In **10a** and **11a** the stacking is of D–A type, in **13a** both D–A and A–A overlaps are present simultaneously. The mean interplanar separations are fairly uniform in **7a** (3.48–3.50 Å), **8a** (3.36–3.46 Å) and **13a** (3.48–3.60 Å), whereas in **10a** these separations alternate between 3.39 and 3.79 Å, that is, the stack effectively consists of dimers. The inter-stack motif is herringbone, except in the triclinic structure of **8a** in which all of the molecules are parallel. Thus, changing the substituents affects the crystal packing, through a change of molecular dimensions and intermolecular interactions S⋯O in **7a**, **8a** and **11a** (3.19 to 3.25 Å), O⋯N in **13a** (2.93 Å) and S⋯S in **8a** (3.54 Å), although these are rather weak. More detailed analysis of the crystal packing in fluorene–dithiole push–pull compounds, which includes dyads **7a**, **8a**, **10a**, **11a** and **13a**, will be published elsewhere.<sup>[40]</sup>

**Theoretical studies:** The geometry and electronic structures of the fluorene–dithiole diads were calculated by using the hybrid B3LYP functional of density functional theory (DFT).<sup>[41]</sup> This level of theory with a medium basis set (6-31G(d)) is now routinely used to study medium-sized organic molecules and has been shown to accurately predict the structure and energy of other related  $\pi$ -functional materials.<sup>[42]</sup>

The calculated gas-phase geometries of **7** to **11** very closely resemble those found in the solid by X-ray crystallography (see above). The difference between the calculated and observed bond lengths of most bonds does not exceed 0.005 to 0.008 Å. The exceptions to this are the C–S bonds in the dithiole ring ( $\Delta = 0.025$ – $0.030$  Å) and the exocyclic C9=C14 bond ( $\Delta = 0.004$ – $0.018$  Å, Table 4). Whereas the small discrepancies in the C–S bond length are possibly owing to intrinsic limitations of the method, the deviations for the C9=C14 bond are likely to be as a result of intermolecular interactions in the solid state. As noted above, the order and the length of this bond is sensitive to the extent of the ICT in the molecules (**1a**↔**1b**). For diads with significant ICT, the resonance input of structure **1b** is substantial, and the partially zwitterionic ground state is highly stabilised by the sur-

rounding dipoles. Thus, compounds **7a** and **8a** with the strongest ICT have the longest C9=C14 bonds, which are further elongated in the solid state (Table 4).

Throughout the range of substituents in the donor and acceptor moieties, the LUMO is almost exclusively localised on the acceptor nitrofluorene moiety (Figure 7). The highest

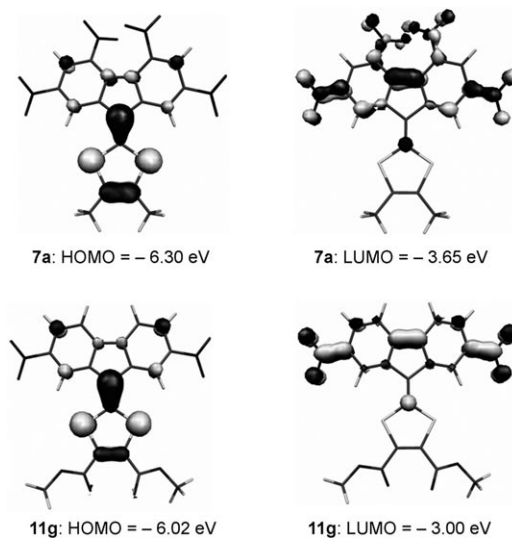


Figure 7. B3LYP/6-31G(d) frontier orbital coefficients in compounds **7a** and **11g**.

LUMO density is seen on the electron-withdrawing substituents and on the C11–C12 bond within this unit. Thus, the reduction potentials of **7** to **11** are predicted to depend strongly on the substituents in the fluorene moiety and be less sensitive to the structure of the dithiole moiety, precisely as was observed in the electrochemical experiments (see above). Conversely, the HOMO is much more delocalised, and is expected to depend strongly on substituents in both the acceptor and donor parts of the molecule. Although the irreversible character of the oxidation process does not allow accurate correlations to be made, a positive shift of 80 mV of the oxidation potential of the 4,5-dimethyl-1,3-dithiole derivatives upon introducing the third nitrogroup in the fluorene moiety (**7d**→**7a**, Table 1) is indicative of this behaviour. The calculated frontier orbital energies (Figure 8) predict that changing the fluorene substitution pattern from two (**7g**) to four (**7a**) nitro groups ( $\Delta\Sigma\sigma_p = 1.56$ ) raises the LUMO by  $\sim 0.8$  eV and HOMO by  $\sim 0.6$  eV, that is, substituents in the fluorene moiety have a slightly larger effect on the LUMOs than on the HOMOs (for series **8a–g** and **11a–g** see the Supporting Information). A similar change in the substituents in the donor dithiole moiety (from **7a** to **11a**,  $\Delta\Sigma\sigma_p = 1.24$ ) decreases the LUMO and HOMO energies by 0.15 and 0.29 eV, respectively (see the Supporting Information). Thus, substituents in the dithiole moiety have a stronger effect on HOMO orbital energies. The calculated orbital energies are within 0.6 eV of values determined by electrochemistry, but surprisingly, even larger differences are found



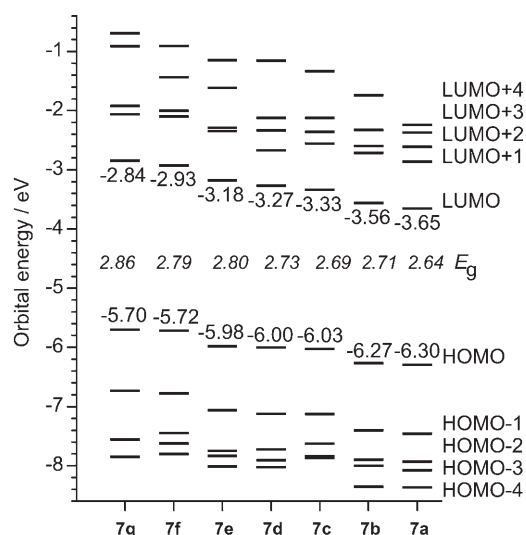


Figure 8. B3LYP/6-31G(d) orbital energy diagram and the HOMO-LUMO gap ( $E_g$ ) for compounds **7a-g**.

for the electrochemical and computed HOMO-LUMO gaps ( $>1$  eV, cf. Table 1 and Figure 8). In part, this is owing to the irreversible character of the oxidation process, which makes it impossible to accurately determine the thermodynamic redox potentials. A much better correlation was observed between the first optical transition (optical gap,  $h\nu_{\text{ICT}}$ ) and the calculated HOMO-LUMO gaps (see the Supporting Information). According to time-dependent (TD) DFT calculations, the lowest energy absorption of compounds **7** to **11** is always a simple HOMO-LUMO transition. The calculated transition energies are in good agreement with the observed  $h\nu_{\text{ICT}}$  values (Figure 9). Remarkably, however, the offset between the experimental and calculat-

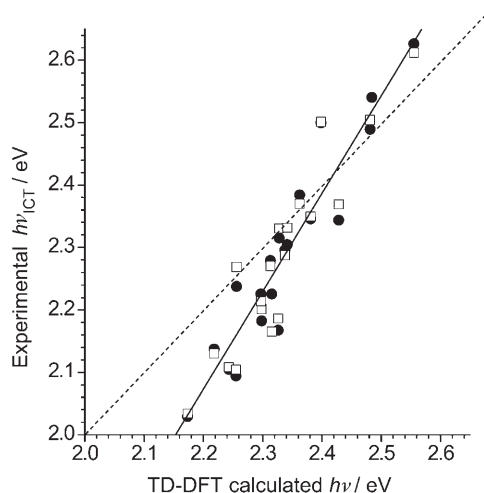
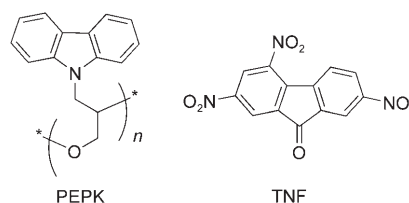


Figure 9. Relationships between the  $h\nu$  calculated from TD-DFT B3LYP/6-31G(d) in the gas phase and experimental  $h\nu_{\text{ICT}}$  energies from electron absorption spectra of compounds **7a-f**, **8a-e.g**, **9a**, **10a** and **11a-e.g** in 1,2-dichloroethane (●) and DMF (□). The dashed line corresponds to a slope of  $45^\circ$  of equal energies, the solid line shows the linear fit for data in 1,2-dichloroethane ( $h\nu_{\text{ICT}} = -(1.37 \pm 0.31) + (1.57 \pm 0.13)h\nu_{\text{TD-DFT}}$ ;  $s_0 = 0.05$ ,  $r = 0.941$ ,  $n = 20$ ).

ed values varies significantly with substituents, and the diads consisting of strong acceptor and donor fragments have an ICT energy that is lower than the calculated value by up to 0.15 eV. This behaviour is consistent with the solvent effects, which should be stronger for compounds with pronounced charge-transfer character.

**Materials applications:** Carbazole-containing polymers are widely used hole-transporting materials with pronounced photoconductivity in the ultraviolet region of the spectrum.<sup>[12,13]</sup> 2,4,7-Trinitrofluorenone (TNF) and 2,4,7-trinitro-9-dicyanomethylene-fluorene (DTF) are known as efficient fluorene acceptors, commercially used as sensitizers of electrophotographic and photothermoplastic materials based on carbazole-containing photoconductive polymers.<sup>[11,43,44]</sup> Thus, PVK/TNF blend was the first commercially used organic material to replace selenium in the electrographic process (IBM Copier I Series, 1970).<sup>[45]</sup> The broad absorption of the PVK/TNF CTC extends the photosensitivity throughout the visible region of the spectrum. However, a low absorptivity of the intermolecular CTC limits the photosensitisation efficiency and requires a high concentration of acceptor units. Furthermore, the spectral zone of the photosensitivity of such materials cannot be easily expanded into the long-wavelength visible and near-IR regions (as required for some applications, for example, holographic interferometry by using He/Ne or solid state NIR lasers). A number of dye molecules dispersed in a polymer matrix (e.g., in PVK or poly(*N*-epoxypropylcarbazole) (PEPK)) have been successfully used as photoreceptors in the electrophotographic process to increase the sensitivity in a certain region of the spectrum (at the absorption maximum of the dye).<sup>[46]</sup> However, they are generally not suitable for photothermoplastic processes owing to poor rheological properties of the films and inefficient thermodeformation during the development of the latent image. On the other hand, the photothermoplastic process has some important advantages over electrophotography (real-time information recording, reversibility of the image formation-erase process, high sensitivity, suitability for hologram recording), and consequently, wider areas of applications (e.g., holographic interferometry). Photothermoplastic storage media (PTSM) based on polymer donor-molecular acceptor CTCs are widely studied in this instance.<sup>[11]</sup> Combining strong absorption and electron affinity in fluorene acceptors with ICT, we hoped to increase the photoresponse of PTSM in the ICT region of the acceptor.

Thus, we have prepared thin films ( $(1.2 \pm 0.1) \mu\text{m}$ ) of the hole-transporting material PEPK blended in different ratios



with fluorene acceptor **6a** and used them as photothermo-plastic storage media. Analogous films have been prepared with TNF, which has an electron affinity very close to that of **6a**, but lacks ICT. Figure 10 shows the spectral distribu-

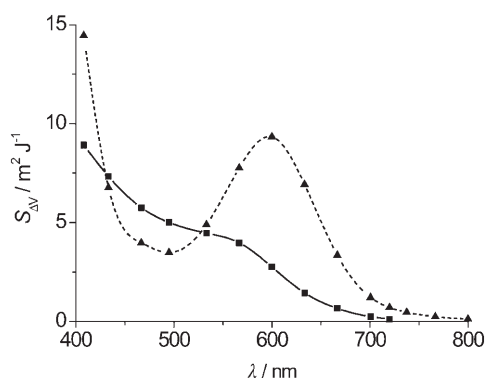


Figure 10. Spectral distribution of the electrophotographic response ( $S_{AV}$ ) of PEPK films sensitised by 5 wt % of acceptors **6a** (▲) and TNF (■).

tion of the electrophotographic response ( $S_{AV}$ ) of PEPK films sensitised by acceptor **6a** in comparison with TNF. Whereas the spectral response of PEPK/TNF films in the electrophotographic regime decreases above approximately 560 nm, PTSM with acceptor **6a** demonstrates an increased response in the region of 500 to 700 nm with a maximum at around 600 nm, which corresponds well to the ICT energy of the acceptor (Table 3). The long-chain  $C_{18}H_{37}$  groups in **6a** substantially increase the solubility of the acceptor and enhance the rheological properties of PTSM, which makes them suitable for hologram recording by using a simple He/Ne laser ( $\lambda = 632.9$  nm) even without the additional plasticiser used in other acceptors (20–30 wt %), such as TNF, to achieve appropriate thermodetormation properties of the films, but which decrease the photoresponse of the material owing to a dilution effect.

In contrast to TNF, for which  $S_{AV}$  decreases with increasing wavelength in the visible region, compound **6a** displays increased sensitivity in its ICT region. At the He/Ne laser wavelength, PEPK/**6a** PTSM achieves an electrophotographic sensitivity approximately five times higher than that of the PEPK/TNF material, even at much lower concentrations of the acceptor (Table 5). The long-chain substituents in **6a** have a pronounced plasticising effect on the PTSM and improve its rheological properties. Even at high concentrations of **6a** (20 wt %), no phase segregation or crystallisation of the acceptor from the blend were observed, which occurs for films

of PEPK or PVK with TNF or DTF at concentrations greater than 10 wt % of the acceptors. This leads to a high diffraction efficiency ( $\eta_{max} = 25\%$ ) that is not far from the theoretical limit for plane light wave holograms (33.9%)<sup>[47]</sup> and allowed the films to attain an extremely high level of holographic sensitivity ( $S_{\eta} = 250\text{--}300\text{ m}^2\text{ J}^{-1}$ , at  $\eta = 1\%$ ). Remarkably, only one to two mol % of **6a** is sufficient to reach the maximum sensitivity of the PTSM. In addition, PTSM with **6a** as an acceptor shows a higher dynamic range of hologram recording compared with TNF, which allows better registration of low-contrast objects. The significant (more than an order of magnitude) increase in the holographic sensitivity and the fact that the spectral response of this sensitivity is linked to a position of the ICT band (and thus can be tuned by substituents) makes this type of acceptor very promising as a sensitizer for recording holograms on PTSM materials.

## Experimental Section

**General:** Acetone, DMF and DMA were purified as described previously.<sup>[48]</sup> Chlorobenzene and 1,2-dichloroethane were stirred with sulfuric acid, washed with water, dried over  $MgSO_4$ , distilled from  $P_2O_5$  and then from CaO. Methyl trifluoromethylsulfonate (methyl triflate,  $\geq 98\%$ , Aldrich) and  $Bu_4NPF_6$  (Fluka, puriss) were used as received. UV/Vis spectra were acquired by using a Varian Cary 5000 UV/Vis-NIR spectrometer. Nitrosubstituted fluorenes **4b,e**<sup>[23]</sup> and **4c,f**<sup>[20]</sup> were prepared by nitration of fluorene or its 4-substituted derivatives with nitric acid or its mixture with acetic or sulfuric acid, as described previously.

**Cyclic voltammetry:** Electrochemical experiments were carried out by using a BAS Epsilon electrochemical analyser. CV was performed in a three-electrode cell equipped with a platinum disk ( $\phi = 1.6$  mm) as the working electrode, platinum wire as a counter electrode and a non-aqueous  $Ag/Ag^+$  reference electrode (0.01 M  $AgNO_3$  and 0.1 M  $Bu_4NPF_6$  in MeCN). Cyclic voltammograms were recorded at room temperature in dry  $CH_2Cl_2$  or DMA, deoxygenated by bubbling with argon gas, with 0.1 M  $Bu_4NPF_6$  as supporting electrolyte. The potentials are given versus ferrocene (Fc), which was used as an internal standard and showed the following potentials against the reference electrode: +0.20 V (vs.  $Ag/Ag^+$  in  $CH_2Cl_2$ ), and +0.10 V (vs.  $Ag/Ag^+$  in DMA).

**X-Ray crystallography:** X-ray diffraction experiments were carried out by using a SMART 3-circle diffractometer with a 1 K CCD area detector and graphite-monochromated  $MoK_{\alpha}$  radiation ( $\lambda = 0.71073$  Å) and a Cryostream (Oxford Cryosystems) open-flow  $N_2$  cryostat. The structures

Table 5. Results of PTSM tests based on PEPK sensitised by fluorene acceptors.

Acceptor	Concentration [wt %] (mol %)	$\lambda = 632.9$ nm					
		$V_0^{[a]}$ [V]	$\Delta V/V_0^{[b]}$ [%]	$S_{AV}^{[c]}$ [ $m^2 J^{-1}$ ]	$S_{\eta}^{[d]}$ [ $m^2 J^{-1}$ ]	$\eta_{max}^{[e]}$ [%]	DR <sup>[f]</sup>
TNF	5.0 (3.5)	210	14	1.9	9	15	1000
<b>6a</b>	2.0 (0.44)	170	10	8	210	$\geq 25$	
<b>6a</b>	5.0 (1.1)	160	10	10	250	$\geq 25$	$\geq 3000$
<b>6a</b>	10 (2.2)	155	10–15	12–16	250–300	25	$\geq 3000$
<b>6a</b>	20 (4.4)	135–140	20–25	10–12	200–250	20	$\geq 2000$

[a]  $V_0$  is the surface potential of the film, charged in the dark. [b]  $\Delta V/V_0$  is the dark decay of the surface potential for 30 s. [c]  $S_{AV}$  is the electrophotographic response of the film estimated by the latent electrostatic image as 20% decay of the surface potential under illumination. [d]  $S_{\eta}$  is the photoresponse estimated by visualised image at the level of diffraction efficiency of the hologram  $\eta = 1\%$ . [e]  $\eta_{max}$  is the maximal diffraction efficiency of the film for plane wave hologram recording. [f] DR is dynamic range of hologram recording, defined as the maximal difference between the intensity of the reference and object laser beams to achieve the diffraction efficiency  $\eta = 1\%$ .

were solved by direct methods and refined by full-matrix least squares against  $F^2$  of all reflections by using SHELXTL software<sup>[49]</sup> (Table 6). CCDC 114934 (**8a** SADWUP), 656461 (**7a**), 656462 (**10a**), 656463 (**11a**) and 656464 (**13a**) contain the supplementary crystallographic data for this paper. These data can be obtained free of charge from The Cambridge Crystallographic Data Centre via [www.ccdc.cam.ac.uk/data\\_request/cif](http://www.ccdc.cam.ac.uk/data_request/cif).

Table 6. Crystal data for compounds **7a**, **10a**, **11a**, and **13a**.<sup>[a]</sup>

Compound	<b>7a</b>	<b>10a</b>	<b>11a</b>	<b>13a</b>
formula	C <sub>18</sub> H <sub>10</sub> N <sub>4</sub> O <sub>8</sub> S <sub>2</sub>	C <sub>18</sub> H <sub>8</sub> N <sub>4</sub> O <sub>9</sub> S <sub>2</sub> ·C <sub>2</sub> H <sub>6</sub> OS	C <sub>20</sub> H <sub>10</sub> N <sub>4</sub> O <sub>12</sub> S <sub>2</sub>	C <sub>20</sub> H <sub>8</sub> N <sub>4</sub> O <sub>8</sub> S <sub>2</sub>
$M_r$	474.42	582.53	562.44	496.42
$T$ [K]	120	105	100	120
$a$ [Å]	10.994(2)	13.4384(14)	10.8860(17)	18.406(2)
$b$ [Å]	9.831(2)	8.0904(8)	27.790(4)	25.936(3)
$c$ [Å]	17.003(3)	21.379(2)	7.2462(12)	8.067(1)
$\beta$ [°]	91.84(1)	99.77(2)	96.18(1)	100.76(4)
$V$ [Å <sup>3</sup> ]	1836.7(5)	2290.7(4)	2179.4(6)	3783.3(8)
$Z$	4	4	4	8
$\mu$ [mm <sup>-1</sup> ]	0.35	0.40	0.33	0.35
reflns collected	22279	27536	19407	27264
reflns unique, $R_{int}$ [%]	4865, 3.5	6118, 3.8	4812, 5.1	8727, 7.3
$R_1$ , $wR_2$ [%]	3.0, 8.1	3.6, 9.3	4.5, 10.8	4.8, 11.0

[a] All compounds are monoclinic with space group  $P2_1/c$  (no. 14).  $R_1 = \sum ||F_o| - |F_c|| / \sum |F_o|$  on the data with  $I > 2\sigma(I)$ .  $wR_2 = \{\sum [w(F_o^2 - F_c^2)^2 / \sum w(F_o^2)^2]\}^{1/2}$ .

**Computational procedures:** DFT computations of the geometries of compounds **7** to **12** were carried out using the Gaussian 03<sup>[50]</sup> package of programs by using Pople's 6-31G split valence basis set supplemented by d-polarisation functions for heavy atoms. Becke's three-parameter hybrid exchange functional<sup>[51]</sup> with Lee–Yang–Parr gradient-corrected correlation functional (B3LYP)<sup>[52]</sup> were employed. Thus, the geometries were optimised at the B3LYP/6-31G(d) level of theory and the electronic structures were calculated at the same level of theory. The lowest energy absorptions were obtained from TD-DFT calculations (at the same B3LYP/6-31G(d) level) for optimised geometries. Contours of HOMO and LUMO orbitals were visualised at a cut-off of 0.05 by using the Molkel v.4.3 program.<sup>[53]</sup>

**Photophysical measurements of sensitised PEPK films:**<sup>[11]</sup> PTSM were prepared in the following way: PEPK (0.5 g) obtained by anionic polymerisation of *N*-(2,3-epoxypropyl)carbazole<sup>[54]</sup> and a corresponding amount of **6a** were dissolved separately in methyl ethyl ketone (both in 5 mL), and then the solutions were combined and filtered. The resulting solution was supported on an ITO-coated glass base. The final thickness of the photoconductive films was  $(1.2 \pm 0.1) \mu\text{m}$ . The surface of the film was charged by a positive corona discharge grid; the final potentials were  $V_0 \approx 120\text{--}160 \text{ V } \mu\text{m}^{-1}$  (measured by the dynamic sonde method). The relative dark decay of the surface potential ( $\Delta V \times 100 / V_0$ ) was estimated for a time of 30 s ( $\Delta V = V_0 - V_t$ , in which  $V_t$  is the charge potential of the surface in the dark after  $\tau = 30$  s) and lies in the range of 10 to 15%. The electrophotographic sensitivity ( $S_{\Delta V}$  [m<sup>2</sup>J<sup>-1</sup>]) was estimated at a level of 20% decay of the initial potential under illumination with wavelengths of 400 to 900 nm and an intensity of  $0.1 \mu\text{W cm}^{-2}$ . Real holographic sensitivity ( $S_h$  [m<sup>2</sup>J<sup>-1</sup>]) was estimated at the level of 1% diffraction efficiency ( $\eta = 1\%$ ) of the visualised image by recording holograms of the planar light wave at the spatial frequency of  $\nu = 450 \text{ mm}^{-1}$  with irradiation of a He/Ne laser ( $\lambda = 632.9 \text{ nm}$ ). The maximal diffraction efficiency, which was achieved without amplification of the hologram recording ( $\eta_{\text{max}}$  [%]), was found to be the ratio of the beam intensity diffracted into the first order of a diffraction to the intensity of the beam grazed on the hologram when the ratio of the intensities of the integrated beams was 1:3. The dynamic range (DR) of the hologram recording was estimated to be a maximal ratio of the reference and object beams for achieving  $\eta = 1\%$ .

**2-Methylthio-1,3-dithiolium triflates 3A–F:** Methyl triflate (3 mmol) was added to a solution of **2A**,<sup>[55]</sup> **2B**,<sup>[56]</sup> **2C**, **2D**, **2E**<sup>[57]</sup> or **2F**<sup>[58]</sup> (2 mmol) in

dry chloroform (10–30 mL), which caused an exothermic reaction. The reaction mixture was stirred at 45 °C for 1 h, then evaporated in vacuum. The product was used in the condensation reactions with the fluorenes without further purification. Triflates **3A–F** can be stored at –20 °C under argon for several weeks without appreciable decomposition.

**2,4,5,7-Tetranitrofluorene 4a:**<sup>[24]</sup> Fuming nitric acid (60 mL,  $d = 1.50 \text{ g cm}^{-3}$ ) was cooled to 0 °C and fluorene (16.6 g, 0.1 mol) was added with intense stirring whilst the temperature was kept below 10 °C. Additional fuming HNO<sub>3</sub> (40 mL) was then added, the mixture was stirred at 60 °C for 1.5 h and the product was left to crystallise. The product was filtered, washed with nitric acid (10 mL,  $d = 1.35 \text{ g cm}^{-3}$ ), then with water until the washings were neutral and then dried to give **4a** (22.05 g, 64%) as a light yellow powder (m.p. 275–276 °C (decomp)) suitable for further syntheses. It can be additionally recrystallised from a minimal amount of fuming nitric acid. M.p. 278–280 °C (decomp); lit. m.p. 275–276 °C (decomp);<sup>[24b]</sup>  $R_f = 0.30$  (SiO<sub>2</sub>, *m*-xylene/dioxane 10:1). <sup>1</sup>H NMR (400 MHz, [D<sub>6</sub>]acetone):  $\delta = 9.07$  (2H, d,  $J = 2.0$  Hz; H-1,8), 8.89 (2H, d,  $J = 2.0$  Hz; H-3,6), 3.58 ppm (2H, s; H-9); <sup>13</sup>C NMR (100 MHz, [D<sub>6</sub>]acetone):  $\delta = 151.1, 147.2, 140.2, 138.1, 126.8$  (CH),

123.5 (CH), 67.7 ppm (CH<sub>2</sub>).

**2,4,7-Trinitrofluorene 4d:**<sup>[25]</sup> Fuming nitric acid (150 mL,  $d = 1.50$ ) was cooled to 0 °C and fluorene (20 g, 0.12 mol) was added with intense stirring over approximately 30 min while the temperature was kept below +5 °C. The mixture was stirred at 0 to +5 °C for 30 min and then poured onto ice (1 kg). The solid was filtered, washed with water until the washings were neutral and then dried to give crude **4d** (33 g, 91%). The crude product was recrystallised twice from acetic acid to give **4d** as yellow crystals (21.5 g, 59%). M.p. 210–211 °C; lit. m.p. 210–211 °C;<sup>[25]</sup>  $R_f = 0.70$  (SiO<sub>2</sub>; benzene/acetone 30:1); <sup>1</sup>H NMR (400 MHz, [D<sub>6</sub>]acetone):  $\delta = 8.91$  (1H, d,  $J = 2.0$  Hz; H-1), 8.86 (1H, d,  $J = 2.0$  Hz; H-3), 8.65 (1H, d,  $J = 2.0$  Hz; H-8), 8.42 (1H, dd,  $J = 8.8, 2.0$  Hz; H-6), 8.28 (1H, d,  $J = 8.8$  Hz;

Table 7. Conditions for the preparation of compounds **6–11**.

	$t^{\text{[a]}}$ [h]	$T$ [°C]	Y1 <sup>[b]</sup> [%]	Y2 <sup>[c]</sup> [%]	M.p. [°C]
<b>6a</b>	2	20	75	50	131–135
<b>7a</b>	1	20	95	90	> 360
<b>7b</b>	3	30	95	90	> 360
<b>7c</b>	15	30	92	86	> 300 (decomp)
<b>7d</b>	20	40	95	91	> 360
<b>7e</b>	22	50	84	81	> 360
<b>7f</b>	25	70	55	51	> 300 (decomp)
<b>8a</b>	1	20	56	40	321–322.5
<b>8b</b>	3	25	100	88	305–310
<b>8c</b>	3.5	20	71	57	240–242
<b>8d</b>	25	60	55	50	248–250
<b>8e</b>	25	70	21	–	296–297.5
<b>8g</b>	1	110	43	11	289–292
<b>9a</b>	2	20	–	75	> 360
<b>10a</b>	1	20	90	–	350 (decomp)
<b>11a</b>	1	20	85	74	282–284
<b>11b</b>	3	20	90	76	278–282
<b>11c</b>	6	25	74	49	258–263
<b>11d</b>	30	50	33	30	248–252
<b>11e</b>	30	65	28	17	283–287

[a] Reaction time. [b] Crude yield. [c] Purified yield after recrystallisation.

Table 8. <sup>1</sup>H NMR data for compounds **6** to **11**.<sup>[a]</sup>

	1-H ( <i>J</i> <sub>1,3</sub> )	8-H ( <i>J</i> <sub>6,8</sub> )	3-H	6-H	5-H ( <i>J</i> <sub>5,6</sub> )	Other signals
<b>6a</b> <sup>[b,c]</sup>		9.12 (d, <i>J</i> = 1.6 Hz)		8.78 (d)	–	3.11 (t, <i>J</i> = 7.2 Hz; 2SCH <sub>3</sub> ), 1.82–1.71 (m; 2CH <sub>2</sub> ) 1.56–1.44 (m; 2CH <sub>2</sub> ), 1.20–1.40 (m; 14CH <sub>2</sub> ) 0.89 (t, <i>J</i> = 6.8 Hz; 2CH <sub>3</sub> )
<b>7a</b> <sup>[c]</sup>		9.20 (brs)		8.70 (brs)	–	2.49 (s; 2CH <sub>3</sub> )
<b>7b</b> <sup>[d]</sup>		9.09 (brs)		8.61 (d, <i>J</i> = 2.0 Hz)	–	2.44 (s; 2CH <sub>3</sub> )
<b>7c</b> <sup>[e]</sup>	9.04br	8.95 (brs)	8.60 (brs)	8.41 (brs)	–	3.86 (s; CO <sub>2</sub> CH <sub>3</sub> ), 2.41 (s; 2CH <sub>3</sub> )
<b>7d</b> <sup>[e]</sup>	8.98 (d, <i>J</i> = 2.0 Hz)	8.82 (d, <i>J</i> = 2.0 Hz)	8.63 (d)	8.37 (dd)	8.79 (d, <i>J</i> = 8.0 Hz)	2.41 (s; 2CH <sub>3</sub> )
<b>7e</b> <sup>[e]</sup>	8.98 (s)	8.82 (s)	8.63 (s)	8.37 (d)	8.79 (d, <i>J</i> = 8.0 Hz)	2.41 (s; 2CH <sub>3</sub> )
<b>7f</b> <sup>[e]</sup>	8.90 (s)	8.77 (s)	8.47 (s)	8.21 (d)	8.53 (d, <i>J</i> = 9.0 Hz)	4.09 (s; CO <sub>2</sub> CH <sub>3</sub> ), 2.38 (s; 2CH <sub>3</sub> )
<b>8a</b> <sup>[f]</sup>		9.31 (s)		9.06 (s)	–	2.92 (s; 2SCH <sub>3</sub> )
<b>8b</b>		8.96 (brs)	8.80 (brs)	8.71 (brs)	–	2.70 (s; 2SCH <sub>3</sub> )
<b>8c</b>	8.80 (brs)	8.71 (brs)	8.60 (brs)	8.38 (brs)	–	3.85 (s; CO <sub>2</sub> CH <sub>3</sub> ), 2.67 (s; 2SCH <sub>3</sub> )
<b>8d</b>	8.79 (d, <i>J</i> = 2.0 Hz)	8.62 (d, <i>J</i> = 2.0 Hz)	8.74 (d)	8.28 (dd)	8.07 (d, <i>J</i> = 8.8 Hz)	2.68 (s; 2SCH <sub>3</sub> )
<b>8e</b>	8.84 (d)	8.69 (d)	8.84 (d)	8.47 (dd)	8.75 (d, <i>J</i> = 8.4 Hz)	2.67 (s; 2SCH <sub>3</sub> )
<b>8g</b> <sup>[f]</sup>		8.40 (d, <i>J</i> = 2.1 Hz)		8.18 (dd)	8.27 (d, <i>J</i> = 8.4 Hz)	2.99 (s; 2SCH <sub>3</sub> )
<b>9a</b>		8.82 (brs)		8.68 (d, <i>J</i> = 1.6 Hz)	–	–
<b>10a</b> <sup>[g]</sup>		8.78 (brs)		8.63 (d, <i>J</i> = 1.8 Hz)	–	8.48 (s; dithiole-H), 3.99 (s; CO <sub>2</sub> CH <sub>3</sub> )
<b>11a</b>		9.85 (brs)		8.70 (brs)	–	3.93 (s; 2CO <sub>2</sub> CH <sub>3</sub> )
<b>11a'</b> <sup>[f]</sup>	9.33 (brs), 9.31 (d, <i>J</i> = 1.6 Hz; <b>11a</b> )			9.17 (brs), 9.09 (d, <i>J</i> = 1.6 Hz; <b>11a</b> )	–	4.71 (s), 4.32 (s; <b>11a</b> )
<b>11b</b>	8.83 (d, <i>J</i> = 1.6 Hz)	8.77 (d, <i>J</i> = 1.6 Hz)	8.76 (d)	8.72 (d)	–	3.95 (s; 2CO <sub>2</sub> CH <sub>3</sub> )
<b>11c</b>	8.80 (d, <i>J</i> = 1.6 Hz)	8.69 (d, <i>J</i> = 1.6 Hz)	8.65 (d)	8.42 (d)	–	3.95 (s, 2CO <sub>2</sub> CH <sub>3</sub> ), 3.85 (s, CO <sub>2</sub> CH <sub>3</sub> )
<b>11d</b>	8.70 (d, <i>J</i> = 2.0 Hz)	8.34 (d, <i>J</i> = 2.0 Hz)	8.56	8.23 (dd)	7.96 (d, <i>J</i> = 9.0 Hz)	3.96 (s, 2CO <sub>2</sub> CH <sub>3</sub> )

[a] Spectra were recorded in [D<sub>6</sub>]DMSO at 300 MHz by using tetramethylsilane as an internal standard at a temperature of 20°C. [b] Recorded in CDCl<sub>3</sub>. [c] Recorded at 50°C. [d] Recorded at 90°C. [e] Recorded at 120°C. [f] Recorded in D<sub>2</sub>SO<sub>4</sub> at 500 MHz. [g] One drop of CF<sub>3</sub>CO<sub>2</sub>D was added to the sample.

H-5), 4.53 ppm (2H, s; H-9); <sup>13</sup>C NMR (100 MHz, [D<sub>6</sub>]acetone): δ = 151.1, 149.4, 149.0, 148.0, 146.0, 142.0, 137.7, 127.0 (CH), 125.2 (CH), 123.7 (CH), 121.3 (CH), 120.0 (CH), 38.4 ppm (CH<sub>2</sub>).

**General method for the preparation of **6** to **11**:** Dithiolium triflate **3A–F** (0.42–0.45 mmol) was added to a solution of fluorene **4a–g** (0.4 mmol) in DMF (2 mL) and the reaction mixture was stirred at 20 to 70°C for 1 to 30 h. The precipitate that formed was filtered, washed successively with DMF, acetone and 2-propanol, and dried in vacuo to give compounds **6** to **11**, which were purified by recrystallisation from DMF. The reaction temperature, time and yields are collected in Table 7. The <sup>1</sup>H NMR spectra of the synthesised compounds are collected in Table 8.

## Acknowledgements

The work in Canada was supported by NSERC Discovery and a DuPont Young Professor award. I.F.P. thanks The Royal Society of Chemistry for the Journals Grant for International Authors supporting his visit to McGill University. The work in Durham was funded by the EPSRC.

- [1] T. Verbiest, S. Houbrechts, M. Kauranen, K. Clays, A. Persoons, *J. Mater. Chem.* **1997**, *7*, 2175–2189.
- [2] a) P. Innocenzi, B. Lebeau, *J. Mater. Chem.* **2005**, *15*, 3821–3831; b) S. R. Marder, *Chem. Commun.* **2006**, 131–134.
- [3] L. R. Dalton, *J. Phys. Condens. Matter* **2003**, *15*, R897–R934.
- [4] a) D. F. Perepichka, I. F. Perepichka, M. R. Bryce, A. J. Moore, N. I. Sokolov, *Synth. Met.* **2001**, *121*, 1487–1488; b) A. J. Moore, A. Chesney, M. R. Bryce, A. S. Batsanov, J. F. Kelly, J. A. K. Howard, I. F. Perepichka, D. F. Perepichka, G. Meshulam, G. Berkovic, Z. Kotler, R. Mazor, V. Khodorkovsky, *Eur. J. Org. Chem.* **2001**, 2671–2687; c) M. R. Bryce, A. Green, A. J. Moore, D. F. Perepichka, A. S. Batsanov, J. A. K. Howard, I. Ledoux-Rak, M. Gonzalez, N. Martin, J. L. Segura, J. Garin, J. Orduna, R. Alcalá, B. Villacampa, *Eur. J. Org. Chem.* **2001**, 1927–1935.
- [5] R. Kannan, G. S. He, T.-C. Lin, P. N. Prasad, R. A. Vaia, L.-S. Tan, *Chem. Mater.* **2004**, *16*, 185–194.
- [6] L. Porrès, O. Mongin, C. Katan, M. Charlot, T. Pons, J. Mertz, M. Blanchard-Desce, *Org. Lett.* **2004**, *6*, 47–50.
- [7] G. S. He, P. P. Markowicz, T.-C. Lin, P. N. Prasad, *Nature* **2002**, *415*, 767–770.
- [8] R. M. Metzger, *Chem. Rev.* **2003**, *103*, 3803–3834.
- [9] G. J. Ashwell, W. D. Tyrrell, A. J. Whittam, *J. Am. Chem. Soc.* **2004**, *126*, 7102–7110.
- [10] W. D. Gill in *Photoconductivity and Related Phenomena*; (Eds.: J. Mort, D. M. Pai) Elsevier, Amsterdam, **1976**, p. 332.
- [11] a) I. F. Perepichka in *NATO Science Series 3 High Technology, Vol. 79: Multiphoton and Light Driven Multielectron Processes in Organics: Materials, Phenomena, Applications* (Eds.: F. Kajzar, M. V. Agranovich), Kluwer Academic Publishers, Dordrecht, **2000**, pp. 371–386; b) I. F. Perepichka, D. D. Mysyk, N. I. Sokolov in *Current Trends in Polymer Photochemistry*, (Eds.: N. S. Allen, M. Edge, I. R. Bellobono, E. Selli), Ellis Horwood, New York, **1995**, pp. 318–327.
- [12] J. V. Grazulevicius, P. Stroehriegl, J. Pielichowski, K. Pielichowski, *Prog. Polym. Sci.* **2003**, *28*, 1297–1353.
- [13] P. M. Borsenberger, D. S. Weiss, *Organic Photoreceptors for Xerography*, Marcel Dekker, New York, **1998**, p. 768.
- [14] I. F. Perepichka, L. G. Kuz'mina, D. F. Perepichka, M. R. Bryce, L. M. Goldenberg, A. F. Popov, J. A. K. Howard, *J. Org. Chem.* **1998**, *63*, 6484–6493.
- [15] a) J. Ortiz, F. Fernández-Lázaro, Á. Sastre-Santos, J. A. Quintana, J. M. Villalvilla, P. Boj, M. A. Díaz-García, J. A. Rivera, S. E. Stepleton, C. T. Cox, Jr., L. Echegoyen, *Chem. Mater.* **2004**, *16*, 5021–5025; b) L. Martín-Gomis, J. Ortiz, F. Fernández-Lázaro, Á. Sastre-Santos, B. Elliott, L. Echegoyen, *Tetrahedron* **2006**, *62*, 2102–2109.
- [16] V. Percec, M. Glodde, T. K. Bera, Y. Miura, I. Shiyonovskaya, K. D. Singer, V. S. K. Balagurusamy, P. A. Heiney, I. Schnell, A. Rapp, H.-W. Spiess, S. D. Hudson, H. Duank, *Nature* **2002**, *419*, 384–387.
- [17] a) Y. Yamamoto, T. Fukushima, Y. Suna, M. Ishii, A. Saeki, S. Seki, S. Tagawa, M. Taniguchi, T. Kawai, T. Aida, *Science* **2006**, *314*, 1761–1764; b) P. H. J. Kouwer, O. van den Berg, W. F. Jager, W. J. Mijss, S. J. Picken, *Macromolecules* **2002**, *35*, 2576–2582.
- [18] a) I. F. Perepichka, A. F. Popov, T. V. Orekhova, M. R. Bryce, A. M. Andrievskii, A. S. Batsanov, J. A. K. Howard, N. I. Sokolov, *J. Org.*



- Chem.* **2000**, *65*, 3053–3063; b) D. F. Perepichka, M. Kondratenko, M. R. Bryce, *Langmuir* **2005**, *21*, 8824–8831.
- [19] a) T. Hansen, J. Becher, *Adv. Mater.* **1993**, *5*, 288–294; b) M. A. Petersen, L. Zhu, S. H. Jensen, A. S. Andersson, A. Kadziola, K. Kilsa, M. B. Nielsen, *Adv. Funct. Mater.* **2007**, *17*, 797–804.
- [20] D. D. Mysyk, I. F. Perepichka, D. F. Perepichka, M. R. Bryce, A. F. Popov, L. M. Goldenberg, A. J. Moore, *J. Org. Chem.* **1999**, *64*, 6937–6950.
- [21] I. F. Perepichka, D. F. Perepichka, M. R. Bryce, L. M. Goldenberg, L. G. Kuz'mina, A. F. Popov, A. Chesney, A. J. Moore, J. A. K. Howard, N. I. Sokolov, *Chem. Commun.* **1998**, 819–820.
- [22] a) Yu. A. Cherkasov, E. L. Alexandrova, M. V. Smirnov, A. I. Rumjantsev, *Opt. Laser Technol.* **1996**, *28*, 291–295; b) Yu. A. Cherkasov, Yu. A. Pryakhin in *Recording Materials for Holographic Imaging and Cine-Holography*, Nauka, Leningrad, **1979**, pp. 119–143 (in Russian).
- [23] D. D. Mysyk, I. F. Perepichka, A. S. Edzina, O. Ya. Neilands, *Latv. Kim. Z.* **1991**, 727–735 (in Russian).
- [24] a) I. F. Perepichka, D. D. Mysyk, USSR 862561, **1981**; b) D. D. Mysyk, I. F. Perepichka, L. I. Kostenko, USSR 1050249, **1983**.
- [25] A. M. Andrievskii, E. I. Sidorenko, V. V. Titov, K. M. Dyumaev, USSR 982322, **1982**.
- [26] N. V. Kravchenko, V. N. Abramov, N. M. Semenenko, *Zh. Org. Khim.* **1989**, *25*, 1938–1945 (in Russian); *Russ. J. Org. Chem.* **1989**, *25*, 1752–1759 (English translation).
- [27] a) P. I. Dem'yanov, G. V. Fedorova, V. S. Petrosyan, O. A. Reutov, *Izv. Akad. Nauk SSSR, Ser. Khim.* **1984**, 2403 (in Russian); *Bull. Acad. Sci. USSR, Div. Chem. Sci.* **1984**, *33*, 2196 (English translation); b) N. M. Semenenko, V. N. Abramov, N. V. Kravchenko, V. S. Trushina, P. G. Buyanovskaya, V. L. Kashina, I. V. Mashkevich, *Zh. Obshch. Khim.* **1985**, *55*, 324–330 (in Russian); *Russ. J. Gen. Chem.* **1985**, *55*, 284–290 (English translation); c) V. N. Abramov, A. M. Andrievskii, N. A. Bodrova, M. S. Borodkina, N. V. Kravchenko, L. I. Kostenko, I. A. Malakhova, E. G. Nikitina, I. G. Orlov, I. F. Perepichka, I. S. Pototskii, N. M. Semenenko, V. S. Trushina, USSR 1343760, **1987**; d) I. N. Chechulina, E. R. Milaeva, Yu. G. Bundel', A. I. Prokofiev, A. M. Andrievskii, K. M. Dyumaev, *Zh. Org. Khim.* **1988**, *24*, 2132–2137 (in Russian); e) D. F. Perepichka, I. F. Perepichka, A. F. Popov, M. R. Bryce, A. S. Batsanov, A. Chesney, J. A. K. Howard, N. I. Sokolov, *J. Organomet. Chem.* **2001**, *637*–639, 445–462; f) I. F. Perepichka, D. F. Perepichka, S. B. Lyubchik, M. R. Bryce, A. S. Batsanov, J. A. K. Howard, *J. Chem. Soc. Perkin Trans. 2* **2001**, 1546–1551.
- [28] a) P. J. Skabara, I. M. Serebryakov, I. F. Perepichka, *J. Chem. Soc. Perkin Trans. 2* **1999**, 505–513; b) P. J. Skabara, R. Berridge, I. M. Serebryakov, A. L. Kanibolotsky, L. Kanibolotskaya, S. Gordyev, I. F. Perepichka, N. S. Sariciftci, C. Winder, *J. Mater. Chem.* **2007**, *17*, 1055–1062.
- [29] The dithiolium salts **3** can be also prepared by treatment of 1,3-dithiol-2-thiones with dimethyl sulphate or methyl iodide, although elevated temperatures are required.
- [30] An alternative protonation of the C14 carbon on the dithiole ring is not expected because it would result in an antiaromatic fluorenum cation; W. C. Herndon, N. S. Mills, *J. Org. Chem.* **2005**, *70*, 8492–8496.
- [31] a) A. S. Benahmed-Gasmi, P. Frère, A. Belyasmine, K. M. A. Malik, M. B. Hursthouse, A. J. Moore, M. R. Bryce, M. Jubault, A. Gorgues, *Tetrahedron Lett.* **1993**, *34*, 2131–2134; b) M. Giffard, P. Alonso, J. Garín, A. Gorgues, T. P. Nguyen, P. Richomme, A. Robert, J. Roncali, S. Uriel, *Adv. Mater.* **1994**, *6*, 298–300; c) M. Giffard, P. Frère, A. Gorgues, A. Riou, J. Roncali, L. Toupet, *J. Chem. Soc. Chem. Commun.* **1993**, 944–945.
- [32] a) M. Bendikov, D. F. Perepichka, F. Wudl, *Chem. Rev.* **2004**, *104*, 4891–4945; b) L. Sánchez, M. A. Herranz, N. Martín, *J. Mater. Chem.* **2005**, *15*, 1409–1421; c) L. Echegoyen, L. E. Echegoyen, *Acc. Chem. Res.* **1998**, *31*, 593–631.
- [33] Calculated from the equation  $E_{1/2} = E_{1/2}^0 + \rho^D \Sigma \sigma_p^D$  (in which  $\sigma_p^D$  is the Hammett constant for the substituents in the dithiole ring).
- [34] a) B. S. Jensen, V. D. Parker, *J. Am. Chem. Soc.* **1975**, *97*, 5211–5217; b) A. Rainis, M. Swarz, *J. Am. Chem. Soc.* **1974**, *96*, 3008–3010.
- [35] S. Amriou, C. Wang, A. S. Batsanov, M. R. Bryce, D. F. Perepichka, E. Ortí, R. Viruela, J. Vidal-Gancedo, C. Rovira, *Chem. Eur. J.* **2006**, *12*, 3389–3400.
- [36] D. F. Perepichka, M. R. Bryce, I. F. Perepichka, S. B. Lyubchik, N. Godbert, C. A. Christensen, A. S. Batsanov, E. Levillain, E. J. L. McInnes, J. P. Zhao, *J. Am. Chem. Soc.* **2002**, *124*, 14227–14238.
- [37] a) D. F. Perepichka, M. R. Bryce, E. J. L. McInnes, J. P. Zhao, *Org. Lett.* **2001**, *3*, 1431–1433; b) D. F. Perepichka, M. R. Bryce, A. S. Batsanov, E. J. L. McInnes, J. P. Zhao, R. D. Farley, *Chem. Eur. J.* **2002**, *8*, 4656–4669.
- [38] C. Hansch, A. Leo, R. Taft, *Chem. Rev.* **1991**, *91*, 165–195.
- [39] a) For a review, see: M. Leclerc, *Adv. Mater.* **1999**, *11*, 1491–1498; b) S. Garreau, M. Leclerc, N. Errien, G. Louarn, *Macromolecules* **2003**, *36*, 692–697.
- [40] L. G. Kuz'mina, A. S. Batsanov, D. F. Perepichka, I. F. Perepichka, unpublished results.
- [41] a) C. Lee, W. Yang, R. G. Parr, *Phys. Rev. B* **1988**, *37*, 785–789; b) A. D. Becke, *J. Chem. Phys.* **1993**, *98*, 5648–5652.
- [42] a) J. M. Gonzales, C. J. Barden, S. T. Brown, P. von Rague Schleyer, H. F. Schaefer III, Q.-S. Li, *J. Am. Chem. Soc.* **2003**, *125*, 1064–1071; b) M. Bendikov, H. M. Duong, K. Starkey, K. N. Houk, E. A. Carter, F. Wudl, *J. Am. Chem. Soc.* **2004**, *126*, 7416–7417; c) S. S. Zade, M. Bendikov, *J. Org. Chem.* **2006**, *71*, 2972–2981.
- [43] a) H. Hoegl, G. Barchietto, D. Tar, *Photochem. Photobiol.* **1972**, *16*, 335–352; b) J. M. Pearson, *Pure Appl. Chem.* **1977**, *49*, 463–477; c) R. Schaffert, *IBM J. Res. Dev.* **1971**, *15*, 75.
- [44] P. M. Borsenberger, D. S. Weiss, *Organic Photoreceptors for Xerography*, Marcel Dekker, New York, **1998** pp. 549–554.
- [45] M. D. Shattuck, U. Vahtra, US 3484327, **1969**.
- [46] P. M. Borsenberger, D. S. Weiss, *Organic Photoreceptors for Xerography*, Marcel Dekker, New York, **1998** pp. 599–671.
- [47] K. S. Pennington, J. S. Harper, *Appl. Opt.* **1970**, *9*, 1643–1650.
- [48] A. J. Gordon, R. A. Ford, *The Chemist's Companion: A Handbook of Practical Data, Techniques and References*, Wiley, New York, **1972**.
- [49] G. M. Sheldrick, SHELXTL, Version 6.14, Bruker AXS, Madison WI (USA), **2003**.
- [50] Gaussian 03, Revision B.04, M. J. Frisch, G. W. Trucks, H. B. Schlegel, G. E. Scuseria, M. A. Robb, J. R. Cheeseman, J. A. Montgomery, Jr., T. Vreven, K. N. Kudin, J. C. Burant, J. M. Millam, S. S. Iyengar, J. Tomasi, V. Barone, B. Mennucci, M. Cossi, G. Scalmani, N. Rega, G. A. Petersson, H. Nakatsuji, M. Hada, M. Ehara, K. Toyota, R. Fukuda, J. Hasegawa, M. Ishida, T. Nakajima, Y. Honda, O. Kitao, H. Nakai, M. Klene, X. Li, J. E. Knox, H. P. Hratchian, J. B. Cross, V. Bakken, C. Adamo, J. Jaramillo, R. Gomperts, R. E. Stratmann, O. Yazyev, A. J. Austin, R. Cammi, C. Pomelli, J. W. Ochterski, P. Y. Ayala, K. Morokuma, G. A. Voth, P. Salvador, J. J. Dannenberg, V. G. Zakrzewski, S. Dapprich, A. D. Daniels, M. C. Strain, O. Farkas, D. K. Malick, A. D. Rabuck, K. Raghavachari, J. B. Foresman, J. V. Ortiz, Q. Cui, A. G. Baboul, S. Clifford, J. Cioslowski, B. B. Stefanov, G. Liu, A. Liashenko, P. Piskorz, I. Komaromi, R. L. Martin, D. J. Fox, T. Keith, M. A. Al-Laham, C. Y. Peng, A. Nanayakkara, M. Challacombe, P. M. W. Gill, B. Johnson, W. Chen, M. W. Wong, C. Gonzalez, J. A. Pople, Gaussian, Inc., Wallingford CT, **2004**.
- [51] a) A. D. Becke, *Phys. Rev. A* **1988**, *38*, 3098–3100; b) A. D. Becke, *J. Chem. Phys.* **1993**, *98*, 5648–5652.
- [52] C. Lee, W. Yang, R. G. Parr, *Phys. Rev. B* **1988**, *37*, 785–789.
- [53] a) P. Flükiger, H. P. Lüthi, S. Portmann, J. Weber, Molekel, Version 4.3, Swiss Center for Scientific Computing, Manno (Switzerland), **2002**, <http://www.cscs.ch/molekel/>; b) S. Portmann, H. P. Lüthi, *Chimia* **2000**, *54*, 766–769.
- [54] J. Inaki, G. Sheibeni, K. Takemoto, *Technol. Rep. Osaka Univ.* **1975**, *25*, 249–253.
- [55] J. P. Ferraris, T. O. Poehler, A. N. Bloch, D. O. Cowan, *Tetrahedron Lett.* **1973**, *14*, 2553–2556.



- [56] G. Steimecke, H. Sieler, R. Kirmse, E. Hoyer, *Phosphorus Sulfur* **1979**, 7, 49–55.
- [57] L. R. Melby, H. D. Hartzler, W. A. Sheppard, *J. Org. Chem.* **1974**, 39, 2456–2458.
- [58] M. Vandevyver, M. Roulliay, J. P. Bourgoïn, A. Barraud, V. Gionis, V. C. Kakoussis, G. A. Mousdis, J.-P. Morand, O. Noel, *J. Phys.Chem.* **1991**, 95, 246–251.
- [59] Based on the  $E_{1/2}=0.67$  V for Fc versus NHE and the absolute potential of  $-4.29$  eV for NHE (in DMF); S. Trasatti, *Pure Appl. Chem.* **1986**, 58, 955–966.

Received: September 14, 2007  
Published online: January 31, 2008